Progress In Electromagnetics Research Letters, Vol. 91, 17–24, 2020

Analysis of Resonant Characteristics of *E*- and *H*-Plane Waveguide Junctions with Local Dielectric Inclusions

Yuriy M. Penkin, Victor A. Katrich, Mikhail V. Nesterenko*, Sergey L. Berdnik, and Natalia K. Blinova

Abstract—A general resonant condition for rectangular waveguide junctions operating in the single mode regime of the main waveguide is formulated based on previously developed mathematical models. We will consider three types of junctions with various side arms: T-oriented semi-infinite waveguide with an impedance end wall, semi-infinite waveguide oriented in line with main waveguide, and infinite perpendicularly oriented waveguide. The main waveguide is coupling with the side arm through a narrow slot, and it has a dielectric inclusion in the coupling region. As a result of the analysis of the resonance characteristics for the indicated types of waveguide devices, the correctness of the application of the general resonance condition is substantiated. The possibility of neglecting the imaginary part of the permittivity of the inclusion material in calculations is confirmed by a satisfactory agreement between the numerical results and experimental data for an isolated inclusion.

1. INTRODUCTION

E- and *H*-plane waveguide junctions are widely used in modern UHF and EHF antenna-waveguide technologies [1–8]. As side arms of the waveguide junctions various electrodynamic volumes can be used: infinite and semi-infinite waveguides, resonators, etc. As well known, waveguide structures operating in beyond-cutoff frequency ranges are characterized by high signal attenuation; therefore, beyond-cutoff waveguide sections have now found only limited application as load elements of high-Q resonators. The interest in the beyond-cutoff waveguides had reappeared due to development of devices capable to concentrate microwave power in a local area. Therefore, they can be applied to study the effect of microwave fields on various substances and biological materials. In this case, it is required to ensure the availability of the irradiated sample during the experiment for monitoring its state or the possibility of its movement along the waveguide. The first requirement can be satisfied by using an open area of the beyond-cutoff rectangular waveguide, excited by a narrow slot.

In any case, the control problem of waveguide devices by a non-mechanical method is still relevant. The impedance coatings of monopole inclusions as control elements of power dividing between the output arms of *E*-plane waveguide T-junction with a slot coupling were proposed in [5]. The use of a dielectric inclusion as an element controlling energy and resonant characteristics of waveguide junctions was proposed to use in [6–8]. However, in these publications, the general condition of the waveguide devices operating in resonant mode was not formulated. This paper is aimed at solution of this problem.

Received 7 February 2020, Accepted 9 April 2020, Scheduled 27 April 2020
* Corresponding author: Mikhail V. Nesterenko (mikhail.v.nesterenko@gmail.com).
The authors are with the Department of Radiophysics, Biomedical Electronics and Computer Systems, V. N. Karazin Kharkiv National University, 4, Svobody Sq., Kharkiv 61022, Ukraine.

2. DIFFRACTION PROBLEM ANALYSIS

Consider three types of waveguide junctions shown in Fig. 1. Let a narrow transverse coupling slot cut in a broad wall of an infinite rectangular waveguide with cross-section $a \times b$ radiate into a side rectangular waveguides with cross-section $a_1 \times b_1$. The slot length and width are $2l$ and d, respectively, and the thickness of waveguide wide wall is h. The walls of the coupling waveguides are perfectly conducting, except for the end wall of the side waveguide in the T-junction (Fig. 1(a)), which is with distributed surface impedance. The side waveguides of all junctions are hollow, while a dielectric inclusion with permittivity $\varepsilon = \varepsilon' - i\varepsilon''$ and permeability $\mu = 1$ is located under the coupling slot in the main waveguide. The inclusion length is c. The main waveguide is excited by H_{10}-wave of unit amplitude propagating from the direction $z = -\infty$. We connect the system of rectangular coordinates (x, y, z) with the main waveguide and with the side ones $(\bar{x}, \bar{y}, \bar{z})$, as shown in Fig. 1.

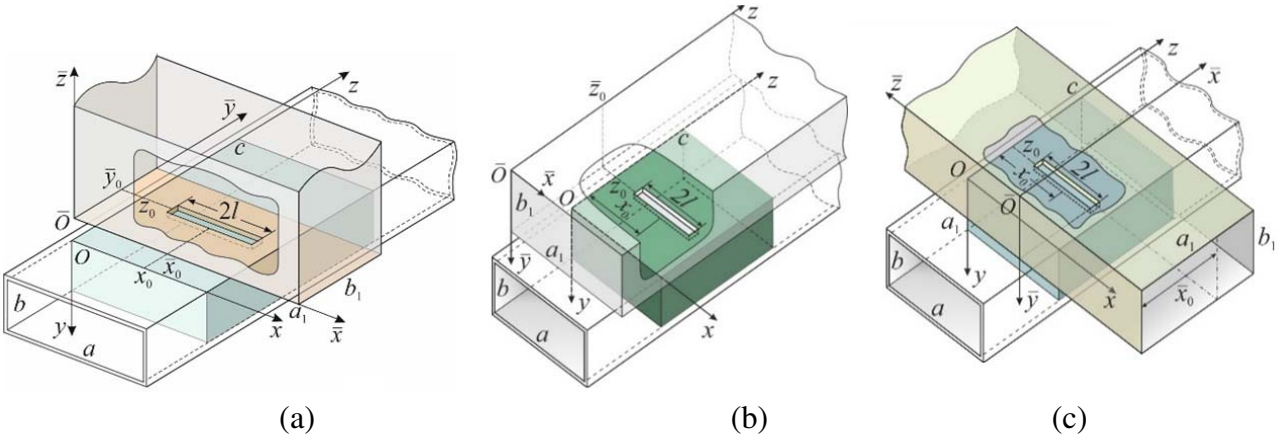

Figure 1. Configuration of the waveguide junctions with local dielectric inclusions: (a) T-junction; (b) directional coupler; (c) cruciform junction.

The unknown field inside the slot can be determined by applying continuity conditions for tangential components of magnetic fields on the slot surfaces $s1$ and $s2$, facing the main "i" and side "e" waveguides which are coupling through the slot cavity "v". The continuity conditions are reduced to two functional equations for the tangential components of the electric field vectors, $\vec{e}_{s1}$ and $\vec{e}_{s2}$, on the slot surfaces:

$$\begin{cases} s1 \Rightarrow \vec{H}^i_\tau(\vec{e}_{s1}) + \vec{H}^i_{0\tau} = \vec{H}^v_\tau(\vec{e}_{s1}) + \vec{H}^v_\tau(\vec{e}_{s2}), \\ s2 \Rightarrow \vec{H}^v_\tau(\vec{e}_{s1}) + \vec{H}^v_\tau(\vec{e}_{s2}) = \vec{H}^e_\tau(\vec{e}_{s2}), \end{cases} \tag{1}$$

where the fields $\vec{H}^i_\tau(\vec{e}_{s1})$, $\vec{H}^e_\tau(\vec{e}_{s2})$, $\vec{H}^v_\tau(\vec{e}_{s1})$, $\vec{H}^v_\tau(\vec{e}_{s2})$ are tangential to the slot plane components in the corresponding electrodynamic volumes, excited by the fields $\vec{e}_{s1}$ and $\vec{e}_{s2}$, and $\vec{H}^i_{0\tau}$ is the tangential component of the magnetic field vector inside the dielectric inclusion not perturbed by the H_{10}-wave incident on the slot.

The system of functional equations (1) can be solved by the method of moments (Galerkin's method). The fields $\vec{e}_{s1}$ and $\vec{e}_{s2}$ can be approximated by a set of vector basis functions

$$\vec{e}_{1q} = \vec{z}^0 \frac{1}{d} \sin \frac{q\pi}{2l}(x - x_0 + l), \quad \vec{e}_{2q} = \vec{\bar{y}}^0 \frac{1}{d} \sin \frac{q\pi}{2l}(\bar{x} - \bar{x}_0 + l) \tag{2a}$$

for waveguide junctions shown in Figs. 1(a) and 1(b), and for the cruciform junction (Fig. 1(c))

$$\vec{e}_{1q} = \vec{z}^0 \frac{1}{d} \sin \frac{q\pi}{2l}(x - x_0 + l), \quad \vec{e}_{2q} = \vec{\bar{x}}^0 \frac{1}{d} \sin \frac{q\pi\bar{z}}{2l}, \tag{2b}$$

where $\vec{x}^0$, $\vec{\bar{y}}^0$, $\vec{z}^0$ are unit vectors of the axes $(x, \bar{y}, z)$, and $q = 1, 2, ..., Q$. If we assume that the field distribution in direction perpendicular to the slot axis is constant, the fields $\vec{e}_{s1}$ and $\vec{e}_{s2}$ can be

represented as follows:

$$\vec{e}_{s1(2)} = \sum_{q=1}^{Q} \dot{V}_{1(2)q} \vec{e}_{1(2)q}. \tag{3}$$

Here $\dot{V}_{1q}$, $\dot{V}_{2q}$ are the unknown complex amplitudes which are solution of a system of linear algebraic equations (SLAE), derived by the Galerkin's method, and in this case takes the form:

$$\begin{cases} \sum\limits_{q=1}^{Q} \dot{V}_{1q} \left(\dot{Y}^{i}_{11,\,pq} + \dot{Y}^{v}_{11,\,pq} \right) + \sum\limits_{q=1}^{Q} \dot{V}_{2q} \dot{Y}^{v}_{12,\,pq} = \dot{F}^{1}_{p}, \\ p = 1, 2, ..., Q, \\ \sum\limits_{q=1}^{Q} \dot{V}_{1q} \dot{Y}^{v}_{21,\,pq} + \sum\limits_{q=1}^{Q} \dot{V}_{2q} \left(\dot{Y}^{v}_{22,\,pq} + \dot{Y}^{e}_{22,\,pq} \right) = 0. \end{cases} \tag{4}$$

The SLAE terms in Eq. (4) have the following dimensions: the matrix elements $\dot{Y}^{i,\,v,\,e}_{mn,\,pq}$ are conductivities; the amplitude coefficients $\dot{V}_{1q}$ and $\dot{V}_{2q}$ are the voltages; the terms $\dot{F}^{1}_{p}$ are magnetomotive forces (MMF). The conductivities and MMF are defined as in [9]. The total field under the slot is represented by the sum of two fields with different structures: the field in an infinite waveguide completely filled with a dielectric and the field caused by multiple reflections at the "dielectric-air" interfaces. The slot conductivities $\dot{Y}^{e}_{22,\,pq}$ in the side waveguide were defined in [6–8]. Here we give an expression $\dot{Y}^{e}_{22,\,pq}$ for the structure shown in Fig. 1(a), which we will need in the future:

$$\begin{aligned} Y^{e}_{22,pq} \;=\; & -\frac{pq}{120\pi a_1 b_1} \left(\frac{\pi}{2l}\right)^2 \sum_{m=0}^{\infty} \sum_{n=0}^{\infty} \frac{(2-\delta_{0m})}{\left(\frac{p\pi}{2l}\right)^2 - \left(\frac{m\pi}{a_1}\right)^2} \frac{(2-\delta_{0n})}{\left(\frac{q\pi}{2l}\right)^2 - \left(\frac{m\pi}{a_1}\right)^2} \\ & \times C_{mn} \left[\bar{Z}_{SW} \gamma_{mn} + \frac{k^2 - (m\pi/a_1)^2}{k} \right] \left[\sin\left(\frac{n\pi d}{2b_1}\right) \Big/ \frac{n\pi d}{2b_1} \right]^2 \cos^2 \frac{n\pi}{b_1} \left(\bar{y}_0 + \frac{d}{2} \right) \\ & \times \left[\sin \frac{m\pi}{a_1} \bar{x}_0 + (-1)^{p+1} \sin \frac{m\pi}{a_1} (\bar{x}_0 + 2l) \right] \left[\sin \frac{m\pi}{a_1} \bar{x}_0 + (-1)^{q+1} \sin \frac{m\pi}{a_1} (\bar{x}_0 + 2l) \right], \end{aligned} \tag{5}$$

where δ_{0m}, δ_{0n} are the Kronecker symbols; $\bar{x}_0$ and $\bar{y}_0$ are the distances between the slot center and the narrow and wide waveguide walls, respectively: $C_{mn} = \frac{k(1+\bar{Z}^2_{SW})}{k\gamma_{mn}(1+\bar{Z}^2_{SW}) + \bar{Z}_{SW}(k^2+\gamma^2_{mn})}$, $\gamma_{mn} = \sqrt{k^2 - (m\pi/a_1)^2 - (n\pi/b_1)^2}$, $k = 2\pi/\lambda$, λ is the wavelength in free space, and $\bar{Z}_{SW} = \bar{R}_{SW} + i\bar{X}_{SW}$ is the complex normalized distributed surface impedance.

Energy characteristics of waveguide devices can be easily determined when unknown amplitudes $\dot{V}_{1q}$ and $\dot{V}_{2q}$ are found as solution of the SLAE in Eq. (4). The reflection coefficient of the dielectric-slot structure in the main waveguide, S_{11}, is defined as the sum of the amplitude of the H_{10}-wave reflected from the dielectric inclusion and the amplitudes of the waves excited by all field harmonics in the slot which propagate in the direction $z < 0$ and pass through the "dielectric-air" interface with the transmission coefficient $T_{-1} = 1 + (\gamma^{\varepsilon}_{10} - \gamma_{10})/(\gamma^{\varepsilon}_{10} + \gamma_{10})$. We can easily obtain that

$$\begin{aligned} S_{11} \;=\; & -\frac{2i\left[(\gamma^{\varepsilon}_{10})^2 - \gamma^2_{10}\right] \sin(\gamma^{\varepsilon}_{10} c)}{(\gamma^{\varepsilon}_{10} + \gamma_{10})^2 e^{i\gamma^{\varepsilon}_{10} c} - (\gamma^{\varepsilon}_{10} - \gamma_{10})^2 e^{-i\gamma^{\varepsilon}_{10} c}} \\ & + \sum_{q=1}^{Q} \frac{4V_{1q} \cdot U_1(q)}{i\omega b d \pi} \sin\left(\frac{\gamma^{\varepsilon}_{10} d}{2}\right) e^{-i\gamma^{\varepsilon}_{10} z_0} \frac{(\gamma^{\varepsilon}_{10} + \gamma_{10}) - (\gamma^{\varepsilon}_{10} - \gamma_{10}) e^{-2i\gamma^{\varepsilon}_{10}(c - z_0)}}{(\gamma^{\varepsilon}_{10} + \gamma_{10})^2 - (\gamma^{\varepsilon}_{10} - \gamma_{10})^2 e^{-2i\gamma^{\varepsilon}_{10} c}}, \end{aligned} \tag{6}$$

where $U_1(q) = \left[\frac{\pi}{a} \cos\frac{q\pi}{2} \sin\left(\frac{\pi l}{a}\right) - \frac{q\pi}{2l} \cos\left(\frac{\pi l}{a}\right) \sin\frac{q\pi}{2}\right] \sin\left(\frac{\pi x_0}{a}\right) \Big/ \left[\left(\frac{\pi}{a}\right)^2 - \left(\frac{q\pi}{2l}\right)^2\right]$, $\gamma_{10} = \sqrt{k^2 - (\pi/a)^2}$, $\gamma^{\varepsilon}_{10} = \sqrt{k^2\varepsilon - (\pi/a)^2}$.

The transmission coefficient S_{12} is calculated by determining the sum of the H_{10}-wave amplitude passing through the inclusion and the amplitudes of the waves excited by all field harmonics in the slot propagating in the direction $z > 0$ which have passed through the "dielectric-air" interface with the coefficient $T_1 = 2\gamma^{\varepsilon}_{10} e^{-i\left(\gamma^{\varepsilon}_{10}-\gamma_{10}\right)c} \Big/ (\gamma^{\varepsilon}_{10}+\gamma_{10})$. Thus, we can write

$$S_{12} = \frac{4e^{-i(\gamma^{\varepsilon}_{10}-\gamma_{10})c}}{(\gamma^{\varepsilon}_{10}+\gamma_{10})^2-(\gamma^{\varepsilon}_{10}-\gamma_{10})^2 e^{-2i\gamma^{\varepsilon}_{10}c}} \times\left\{\gamma_{10}\gamma^{\varepsilon}_{10}+\sum_{q=1}^{Q}\frac{V_{1q}\cdot U_1(q)}{i\omega\mu bd\pi}\sin\left(\frac{\gamma^{\varepsilon}_{10}d}{2}\right)\left[(\gamma^{\varepsilon}_{10}-\gamma_{10})e^{-i\gamma^{\varepsilon}_{10}z_0}-(\gamma^{\varepsilon}_{10}+\gamma_{10})e^{i\gamma^{\varepsilon}_{10}z_0}\right]\right\}. \quad (7)$$

The power transfer coefficient to the upper waveguide $|S_e|^2$ can be found by the formula

$$|S_e|^2 = \frac{2}{\omega b\gamma_{10}\pi^2/a_1}\mathrm{Re}\sum_p\sum_q \dot{V}_{2p}\dot{V}^*_{2q}Y^e_{pq}, \quad (8)$$

where sign "$*$" means the complex conjugate.

In [6–9], the resonant condition for the waveguide junction operations was not formulated. If the wall between the coupling waveguides is infinitely thin, the resonant condition can be obtained by using in Eq. (3) only one approximating function. Usually, this condition is reduced to

$$\mathrm{Im}\left(\dot{Y}^i_{11,\,11}+\dot{Y}^e_{22,\,11}\right)=0. \quad (9)$$

Of course, the requirement in Eq. (9) becomes inapplicable to arbitrary thickness of the waveguide walls and function systems in Eq. (3). Then, the resonant condition should be formulated based on other approaches, such as an input impedance concept of waveguide junctions.

In [10], the correctness of the expansion

$$S_{11}=\frac{Z-Z_0}{Z+Z_0}, \quad (10)$$

valid for dielectrics inclusions with material parameters $\varepsilon=\varepsilon'-i\varepsilon''$, $\mu=\mu'-i\mu''$ placed in rectangular waveguides was proved. In Equation (10), Z is the wave impedance of the waveguide filled with the dielectric material, and $Z_0 = 120\pi/\sqrt{1-(\lambda/2a)^2}$ is the wave impedance of a hollow waveguide operating in the single-mode regime. From Eq. (10), it is not difficult to obtain

$$Z = Z_0\frac{1+S_{11}}{1-S_{11}}. \quad (11)$$

Formula (11) can also be applied to the junctions if the inclusion area including the coupling slot in the main waveguide can be interpreted as a volume filled with a dielectric with effective material parameters $(\varepsilon_{ef};\mu)$. Then, it is possible based on Eq. (11) to express the resonance condition in the traditional for the electrodynamics theory form

$$\mathrm{Im}\left(\frac{1+S_{11}}{1-S_{11}}\right)=\chi=0, \quad (12)$$

where S_{11} can be determined by Equation (6) with parameters $(\varepsilon_{ef};\mu)$. Of course, to find $\varepsilon_{ef}=\varepsilon'_{ef}-i\varepsilon''_{ef}$ from the solution of the inverse problem is no less difficult problem than solving the direct diffraction problem. However, in the resonant mode, we can assume that the radiated energy loss through the slot into the adjacent waveguide can be defined only by the imaginary part of the effective permittivity ε''_{ef}. Then, we can suppose that substituting $\varepsilon'_{ef}\approx\varepsilon'$ into the relation (12) is applicable, that is, the resonant condition in Eq. (12) is valid if $\varepsilon'_{ef}\approx\varepsilon'$. Next, we confirm the hypothesis put forward by the results of numerical simulation.

3. NUMERICAL AND EXPERIMENTAL RESULTS

Formulated condition in Eq. (12) is a multi-parameter transcendental equation with respect to the resonant wavelength λ_{res}. Undoubtedly, its solution is much more complicated in the case of a complex value of the permittivity, since the remaining input parameters of the equation are real values. This situation can be avoided if we neglect (due to smallness) the influence of the values of the imaginary parts $\varepsilon''(\varepsilon''_{ef})$ on λ_{res}.

Indeed, according to the results of numerical simulation, the value λ_{res} turns out to be almost independent of the choice of the imaginary part of the permittivity (which corresponds to general physical principles). This conclusion is confirmed by those results presented in Fig. 2 and Fig. 3. Fig. 2 shows the range of energy characteristics ($|S_{11}|^2$ and $|S_{12}|^2$) for insulated inclusions of epoxy-resin, which are characterized by relatively large losses, $\varepsilon = 3.0 - i0.105$. We note that in both cases, the extrema of the dependences of the energy coefficients coincide in frequency, and the amplitudes of the transformation of the dependences decrease. However, in the vicinity of resonances of minimal wave reflection from the inclusion, the values $|S_{11}|^2$ increase with increasing losses in the dielectric. This is due to a decrease in the amplitude of the secondary wave that has passed through the inclusion and quenches the incident wave.

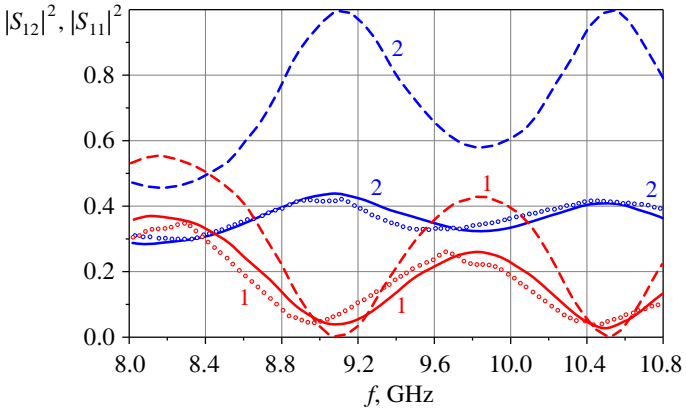

Figure 2. The dependences of energy coefficients for the isolated (without slot) inclusions at $a = 23\,\text{mm}$, $b = 10\,\text{mm}$, $c = 54\,\text{mm}$: $|S_{11}|^2$ — curves 1, $|S_{12}|^2$ — curves 2; solid — $\varepsilon = 3.0 - i0.105$, dashed — $\varepsilon = 3.0$, circles — experimental data.

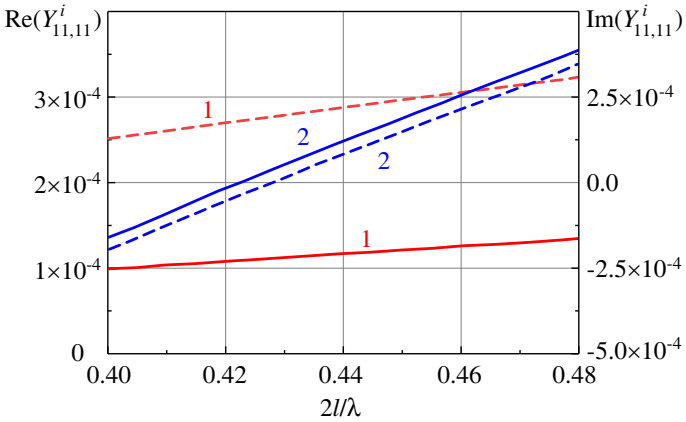

Figure 3. The curves of the real and imaginary parts of the slot conductivity as functions of slot length at $a = 23\,\text{mm}$, $b = 10\,\text{mm}$, $\lambda = 42\,\text{mm}$, $d = 1.0\,\text{mm}$, $z_0 = 2.0\,\text{mm}$, $c = 17.5\,\text{mm}$: $\mathrm{Re}(\dot{Y}^i_{11,11})$ — curves 1, $\mathrm{Im}(\dot{Y}^i_{11,11})$ — curves 2; solid — $\varepsilon = 1.2 - i0.05$, dashed — $\varepsilon = 1.2$.

Figure 3 shows the dependences of the real and imaginary components of the partial conductivity of the slot $\dot{Y}^i_{11,\,11}$ in the waveguide with a dielectric inclusion, calculated by the formula [9]:

$$
\begin{aligned}
Y^i_{11,\,pq} \;=\; & \frac{2}{i\omega\mu_0 abd^2}\sum_{m=1}^{\infty}\sum_{n=0}^{\infty}\frac{(2-\delta_{0n})U_m(q)U_m(p)}{(\gamma^{\varepsilon}_{mn})^3}\left[k^2\varepsilon-\kappa_m^2\right] \\
& \cdot\left(d\gamma^{\varepsilon}_{mn}-\sin\gamma^{\varepsilon}_{mn}d+2i\left(\sin\frac{\gamma^{\varepsilon}_{mn}d}{2}\right)^2\right)-\frac{4}{abd^2}\sum_{m,\,n}\frac{(2-\delta_{0n})}{\gamma^{\varepsilon}_{mn}}\cdot\frac{U_m(q)U_m(p)}{\kappa_m^2+\kappa_n^2}\left(\sin\frac{\gamma^{\varepsilon}_{mn}d}{2}\right)^2 \\
& \cdot\left\{\kappa_m^2\frac{R^M_{-\mu}}{\omega\mu}\times\frac{e^{-2i\gamma^{\varepsilon}_{mn}(c-z_0)}-2R^M_{-\mu}e^{-2i\gamma^{\varepsilon}_{mn}c}+e^{-2i\gamma^{\varepsilon}_{mn}z_0}}{1-R^M_{\mu}R^M_{-\mu}}+\kappa_n^2\frac{\omega\varepsilon R^e_{-\mu}}{(\gamma^{\varepsilon}_{mn})^2}\right. \\
& \left.\cdot\frac{e^{-2i\gamma^{\varepsilon}_{mn}(c-z_0)}+2R^e_{-\mu}e^{-2i\gamma^{\varepsilon}_{mn}c}+e^{-2i\gamma^{\varepsilon}_{mn}z_0}}{1-R^e_{\mu}R^e_{-\mu}}\right\},
\end{aligned}
\tag{13}
$$

where $p=q=1$, $\gamma^{\varepsilon}_{mn}=\sqrt{k^2\varepsilon-\kappa^2}$, $\kappa^2=\kappa_m^2+\kappa_n^2$, $\kappa_m=m\pi/a$, $\kappa_n=n\pi/b$,
$R^e_{-\mu}=\frac{\gamma^{\varepsilon}_{mn}-\varepsilon\gamma_{mn}}{\gamma^{\varepsilon}_{mn}+\varepsilon\gamma_{mn}}$, $R^M_{-\mu}=\frac{\gamma^{\varepsilon}_{mn}-\gamma_{mn}}{\gamma^{\varepsilon}_{mn}+\gamma_{mn}}$, $R^{e(M)}_{\mu}=R^{e(M)}_{-\mu}e^{-2i\gamma^{\varepsilon}_{mn}c}$,
$U_m(v)=\left[\kappa_m\cos\frac{v\pi}{2}\sin(\kappa_m l)-\frac{v\pi}{2l}\cos(\kappa_m l)\sin\frac{v\pi}{2}\right]\sin(\kappa_m x_0)\Big/\left[\kappa_m^2-(v\pi/(2l))^2\right]$.

As can be seen from Fig. 3, if the losses in the dielectric are taken into account, the values $\mathrm{Re}(\dot{Y}^i_{11,\,11})$ change substantially, in contrast to the values $\mathrm{Im}(\dot{Y}^i_{11,\,11})$ for which the changes turn out to be small.

Such changes in the type of dependences of the imaginary part of the conductivity are associated with a manifesting effect, similar to the imperfect "quenching" of the incident wave, in the region of the slot. Moreover, for fixed z_0 and d there is a shift in the frequency range of the resonant length of the slot (when $\mathrm{Im}(\dot{Y}^i_{11,\,11})\to 0$). As shown in the simulation results, for dielectric loss tangent satisfying the inequality $\mathrm{tg}\delta=\frac{\varepsilon''}{\varepsilon'}\le 0.1$, this shift does not exceed 1% of the value λ_{res}. We note that such a numerical estimate is comparable in magnitude with the accuracy of calculating the value of the imaginary part of the slot conductivity [9]. Thus, for dielectrics with $\mathrm{tg}\delta\le 0.1$ an accuracy of determination λ_{res} from condition (12) in the approximation $\varepsilon'_{ef}\approx\varepsilon'$ it turns out to be a limited interval $\pm 0.01\lambda_{res}$.

The obtained estimate of the accuracy of determination λ_{res} was confirmed by numerical studies for all three types of waveguide junctions, whose configurations are presented in Fig. 1. For example, Fig. 4 shows the results of calculations of the energy characteristics for the T-junction (Fig. 1(a)). For the main waveguide with a dielectric inclusion ($\varepsilon=1.2$), the parameters are stored as in Fig. 3, and for the side waveguide section with an ideally conducting end, the following parameters were adopted: $a_1=23\,\mathrm{mm}$, $b_1=10\,\mathrm{mm}$, $x_{01}=a_1/2$, $y_{01}=b_1/2$.

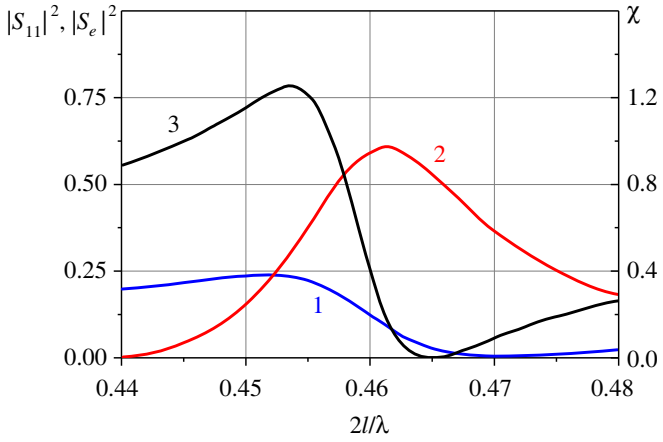

Figure 4. The energy characteristics of the T-junction as functions of slot electrical length: $|S_{11}|^2$ — curve 1, $|S_e|^2$ — curve 2, χ — curve 3.

It should be noted that the use of the approximation $\varepsilon'_{ef} \approx \varepsilon'$ here, which essentially ignores the possibility of correctly taking into account the internal losses in the waveguide device, does not allow us to directly consider cases $\bar{R}_{SW} > 0$ for coating the end of the side waveguide in the T-junction. However, for variants of purely imaginary impedance $\bar{Z}_{SW} = i\bar{X}_{SW}$, by changing the value of which the level of transmitted power to the side waveguide can be adjusted [7], the method proposed above (within the established limits) can be successfully applied. In confirmation of this Fig. 5 presents the results of calculations of the characteristics of T-junctions for the cases of impedance ends of the side waveguides with $\bar{Z}_{SW} = i0.03$ (Fig. 5(a)) and $\bar{Z}_{SW} = i0.05$ (Fig. 5(b)). In the first case, the value of the dielectric constant of the inclusion was assumed to be equal $\varepsilon = 1.13$, and in the second — $\varepsilon = 1.12$ (the remaining parameters of the junction were saved as for Fig. 3).

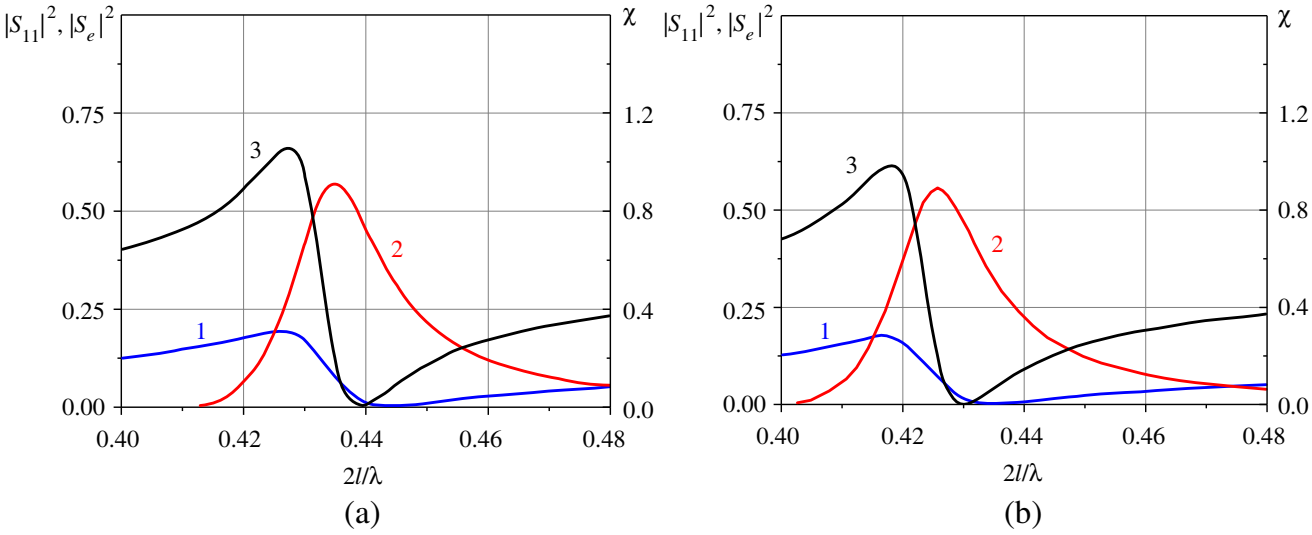

Figure 5. The energy characteristics of the T-junction as functions of slot electrical length: $|S_{11}|^2$ — curve 1, $|S_e|^2$ — curve 2, χ — curve 3. (a) $\bar{Z}_{SW} = i0.03$, $\varepsilon = 1.13$; (b) $\bar{Z}_{SW} = i0.05$, $\varepsilon = 1.12$.

4. CONCLUSION

Models of waveguide devices [6–8], containing a dielectric inclusion in the main waveguide in the region of the coupling slot, allow one to study the energy characteristics of the junctions of rectangular waveguides with different cross-sections, provided that the main waveguide operates in a single mode. It was found that for a given wavelength, the selection of the electrical parameters of the waveguide devices (any of the types considered) can provide, in the interval $0 \le |S_e|^2 \le 0.84$, the required level of power transfer from the main waveguide to the side. It is also shown that regulation over a wide range of the level of power transfer to the side waveguide can be ensured by changing both the value of the permittivity of the inclusion and the value of the impedance distributed at the end of the side waveguide. Regardless of the electrodynamic type of the lateral volume, small changes in the permittivity of the inclusion (of the order of several percent) are sufficient to control the level of power transfer within.

The resonance characteristics of waveguide junctions with local dielectric inclusions are analyzed. A general resonance condition is formulated for a number of waveguide junctions in the range of single mode operation of the main rectangular waveguide containing a dielectric inclusion in the region of the coupling slot. Based on numerical modeling, it was found that for dielectrics with dielectric loss tangent $\mathrm{tg}\delta \le 0.1$, the accuracy of determining the resonant wavelength λ_{res} from the resonance condition in the approximation $\varepsilon_{ef} \approx \varepsilon'$ is limited to $\pm 0.01\lambda_{res}$.

REFERENCES

1. Arndt, F., I. Ahrens, U. Papziner, U. Wiechmann, and R. Wilkeit, "Optimized E-plane T-junction series power dividers," *IEEE Trans. Microwave Theory Tech.*, Vol. 35, 1052–1059, 1987.
2. Yao, H.-W., A. E. Abdelmonem, J.-F. Liang, X.-P. Liang, K. A. Zaki, and A. Martin, "Wide-band waveguide and ridge waveguide T-junctions for diplexer applications," *IEEE Trans. Microwave Theory Tech.*, Vol. 41, 2166–2173, 1993.
3. Widarta, A., S. Kuwano, and K. Kokubun, "Simple and accurate solutions of the scattering coefficients of E-plane junctions in rectangular waveguides," *IEEE Trans. Microwave Theory Tech.*, Vol. 43, 2716–2718, 1995.
4. Abdelmonem, A., H.-W. Yao, and K. A. Zaki, "Slit coupled E-plane rectangular T-junctions using single port mode matching technique," *IEEE Trans. Microwave Theory Tech.*, Vol. 42, 903–907, 1994.
5. Berdnik, S. L., V. A. Katrich, M. V. Nesterenko, and Yu. M. Penkin, "Waveguide T-junctions with resonant coupling between sections of different dimensions," *International Journal of Microwave and Wireless Technologies*, Vol. 9, 1059–1065, 2017.
6. Penkin, Yu. M., S. L. Berdnik, V. A. Katrich, and M. V. Nesterenko, "Waveguide junction with controllable power division," *2016 9th International Kharkiv Symposium on Physics and Engineering of Microwaves, Millimeter and Submillimeter Waves*, 1–4, Kharkiv, Ukraine, 2016.
7. Penkin, Yu. M., S. L. Berdnik, V. A. Katrich, M. V. Nesterenko, and S. V. Pshenichnaya, "Energy characteristics of a T-shaped waveguide junction with a dielectric insert," *2016 8th International Conference on Ultrawideband and Ultrashort Impulse Signals*, 73–76, Odessa, Ukraine, 2016.
8. Penkin, Yu. M., S. L. Berdnik, V. A. Katrich, and M. V. Nesterenko, "Influence of a dielectric insert on energy characteristics of a cruciform waveguide junction," *2016 XXIst International Seminar/Workshop on Direct and Inverse Problems of Electromagnetic and Acoustic Wave Theory*, 42–45, Tbilisi, Georgia, 2016.
9. Penkin, D. Yu. and L. P. Yatsuk, "Analysis of energy characteristics of the transversal slot in a wide wall of a rectangular waveguide with local dielectric inclusion," *Telecomm. Radio Eng.*, Vol. 73, 669–680, 2014.
10. Parkhomenko, M. P., D. S. Kalenov, I. S. Eremin, A. Fedoseev N.A., V. M. Kolesnikova, and Yu. L. Barinov, "Waveguide method for measuring electromagnetic parameters of materials in the microwave range and estimating the measurement error," *Journal of Radio Electronics*, Vol. 9, 1–19, 2018, available at: http://jre.cplire.ru/jre/sep18/6/text.pdf.